Full Wave Analysis and Design of RF Tunable Filters

Jian Xu, Xiao-Peng Liang, Khosro Shamsaifar

Paratek Microwave Inc. 6935-N Oakland Mills Road, Columbia, MD 21045 USA

***Abstract* — In this paper, a systematic design method for the finline structure tunable filter is presented based on filter synthesis and the full wave analysis using Ansoft EM simulation software HFSS. The varactor effects have been discussed. Two filter examples, one in Ka- and the other in K-band, are built and tested to verify the design. The measurement results are in agreement with the simulations.**

I. INTRODUCTION

With the development of the (Ba,Sr)TiO3 (BSTO) films at microwave frequencies, more and more efforts have been focused on applications in the wireless industry. One important application using BSTO material is the RF tunable filter [1]. There have been some papers that introduced the implementation of the BSTO films to the finline waveguide structure to realize the RF filter electric tuning. However, the design methods in those papers are based on the equivalent circuits and are very preliminary. In this paper, a systematic design method for the finline structure tunable filter is presented based on filter synthesis and the full wave analysis using Ansoft EM simulation software HFSS. A two-pole filter example working at 38 GHz is built to verify the design. The measurement results are in excellent agreement with the simulation. Another filter in K-band is presented as well.

II. THEORIES

Like most of the other filter designs, the tunable filter design starts with the synthesis.

A. Synthesis

The filter synthesis usually begins with the transmission response. The most commonly used transmission function is the Chebychev response. The generic features of equiripple amplitude in-band characteristics, together with the sharp cutoffs at the edge of the passband and the high selectivity, give an acceptable compromise between lowest signal degradation and highest noise/interference rejection. The Chebychev transmission response is expressed as:

$$S_{21}^2(s) = \frac{1}{1+e^2 F_N^2(s)} \qquad (1)$$

where $F_N(s)$ is the Chebychev function and ε is the constant related to the return loss. Given the Chebychev order N and the passband equiripple level, the coefficients of the Chebychev polynomials can be determined [2].

The next step is the construction of the general ABCD matrix. Assuming there is no transmission zero, the numerator of the transfer function S21 (s) will be unity and the transfer function becomes:

$$S_{21}(s) = \frac{1}{e_0(s-p_1)(s-p_2)\cdots(s-p_N)} \qquad (2)$$

Where e_0 is the constant normalizing the amplitude of $S_{21}(s)$ to unity. After the S parameters are determined, the ABCD matrix elements can be obtained by the well-known formulas.

The final step of the filter synthesis is to extract the network elements from the ABCD matrix and to obtain the coupling matrix.

B. Filter element design

In the filter synthesis, the resonant frequency, transmission response, and the coupling matrix are obtained. To realize the theoretical response by using the finline waveguide structure, the filter elements must be designed. There are three major structures: the finline waveguide resonator structure, the input & output coupling structure and the mutual coupling structure.

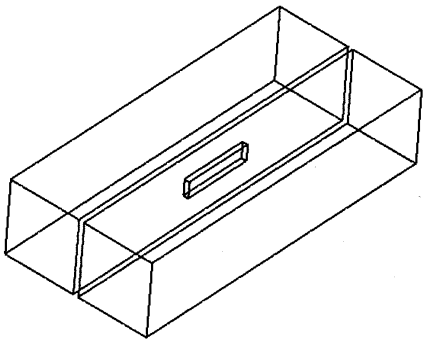

Fig. 1. Finline waveguide resonant structure.

Fig. 1 shows the finline waveguide structure. By running this model in HFSS to search the eigenmode solution, the resonant frequency of the dominant mode will be defined.

The next step is to setup the external Q of the resonator. It is usually called the input or output coupling bandwidth because it is easy to measure. Fig. 2 shows the transition of waveguide to this finline structure.

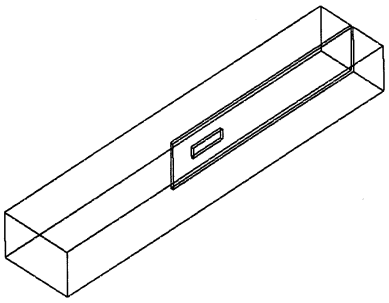

Fig. 2. Simulation model for the input & output coupling.

It can be seen that the waveguide end is the input port and the other end with finline septum is set to be shorted. In this HFSS model, the S11 at the waveguide port is calculated. Fig. 3 shows its phase response. The distance between the phase +90° and -90° will be the input or output coupling bandwidth [3]. In this case, the input coupling bandwidth is (38.738 – 38.490) GHz = 248 MHz.

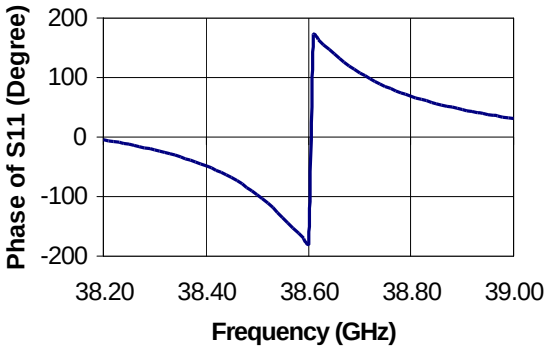

Fig. 3. S11 phase response of the input & output port.

Next is the calculation of the mutual coupling between two resonators. It is also defined as the coupling bandwidth that is easy to measure and simulate [4].

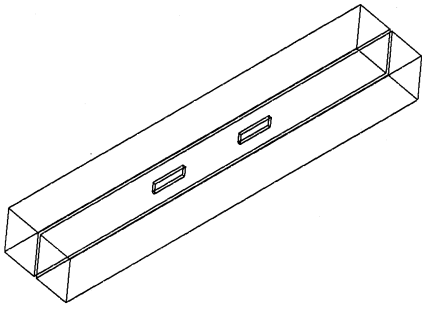

Fig. 4. Simulation model for the mutual coupling.

Fig. 4 shows the model to define the mutual coupling between two finline resonators. Both ends are shorted. We analyze this structure in HFSS by using eigenmode solution. It will be found that the dominant mode splits into two frequencies, one of these is higher than the original resonant frequency and another one is lower than the original frequency. The mutual coupling bandwidth is the difference between these two frequencies.

C. Optimizing the filter by numerically tuning

After we complete the filter element design, the next step is to integrate these elements together as a filter. Fig. 5 is a two pole filter example.

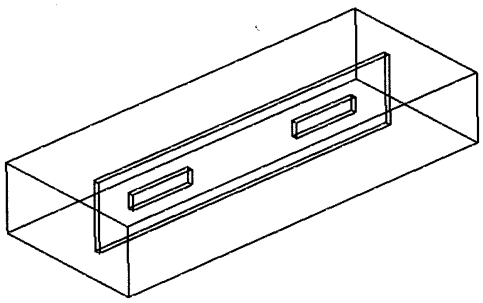

Fig. 5. The two pole finline filter structure.

The input and output ports are the two ends of the waveguide. Analyzing this structure in HFSS by using driving solution and finely tuning the dimensions of each element, we can finally get the designed filter responses.

D. The implementation of the tunable varactors

One common way to add tunable varactors to this finline structure is shown in Fig. 6. At the end of each resonator, a vertical slot is opened, and varactors are placed across these vertical slots, so the DC bias voltage can be added.

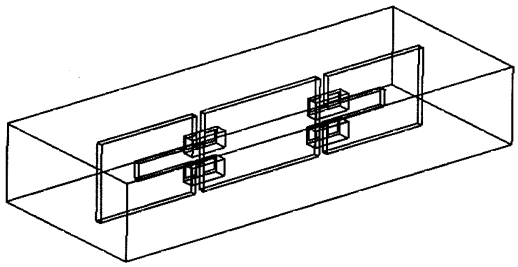

Fig. 6. The two pole finline filter structure with varactors.

In the equivalent circuit, this varactor structure can be simplified as the resonant circuit with loaded capacitances at the ends. If the tunable resonant slot length is kept the same as the one without varactors, the resonant frequency will be. The decrease in resonant frequency will depend on the capacitance value of the varactors. With increase of the

DC bias voltage applied across the varactors, their capacitances will become smaller, so the resonant frequency of the filter will go higher. Fig. 7 shows the typical varactor capacitance change vs. voltage.

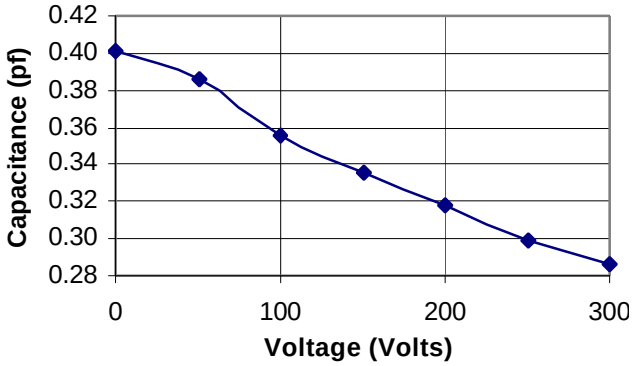

Fig. 7. Typical varactor performance

The varactors effect not only the resonant frequency, but also the external coupling and the mutual coupling of the finline elements. Another paper by the authors will discuss these effects as well as how to include them in the tunable filter design.

III. Examples and Measurement

In this section, a two pole tunable filter working at Ka-band is demonstrated. A three-pole filter at K-band is also introduced.

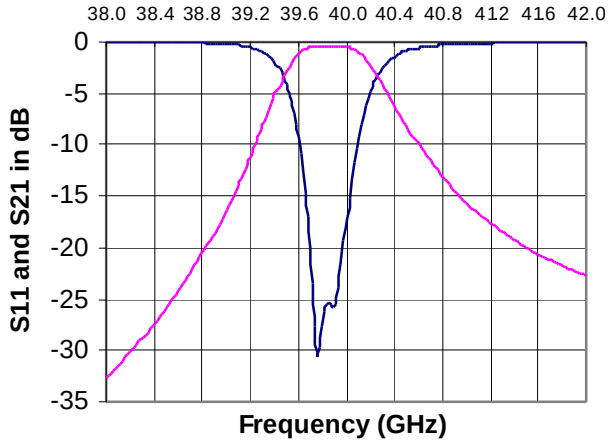

Fig. 8. The HFSS simulation results of the 2 pole filter without varactors.

The two-pole filter structure is shown in Fig. 5. WR28 waveguide is selected for this filter. The thickness of the septum in the middle of the waveguide is 10 mils. The length of the resonator slot is 122 mils. The HFSS simulated filter response is shown as Fig. 8.

From Fig. 8, it can be seen that the center frequency is at 39.8 GHz. BSTO varactors are then added to the simulation model. The thickness of the tunable material is 8 μm and the thickness of the base material (MgO) is 20 mils. The width of the gold pad is 3 mils and the gap between two gold electrodes is 20 μm. These varactors will contribute an average of 0.2 pf of capacitance. Fig. 9 shows the HFSS simulation of the tunable filter responses. It can be seen that the center frequency is lowered to 38.45 GHz.

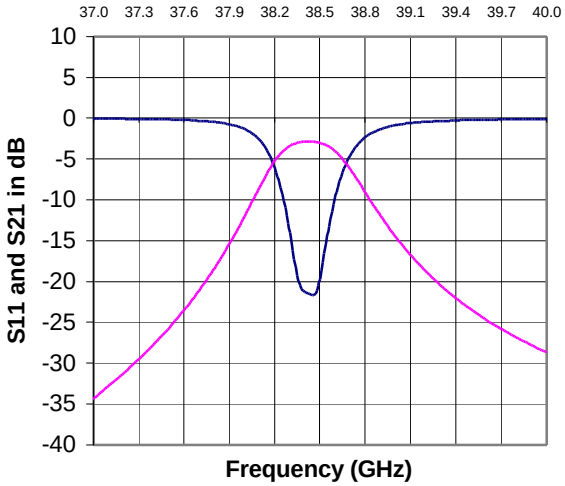

Fig. 9. The HFSS simulation results of the 2 pole filter including varactors.

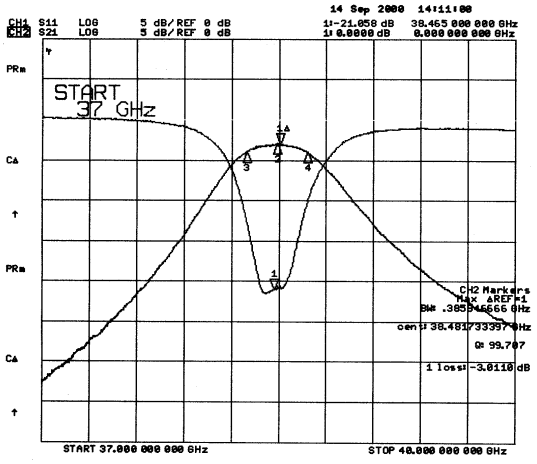

Fig. 10. The measurement results of the 2 pole filter with varactors.

Fig. 10 is the two-pole filter measurement results from the HP8722 network analyzer. No DC bias voltages were added for this measurement. The measured center frequency is 38.48 GHz, which is very close to the simulated results of 38.45 GHz.

To show the tunability of this filter, Fig. 11 & 12 are the filter responses at 100 V and 200V. The original memory curves are the filter responses at 0 V. It can be clearly seen that the tunability of the filter is 408 MHz / 200V.

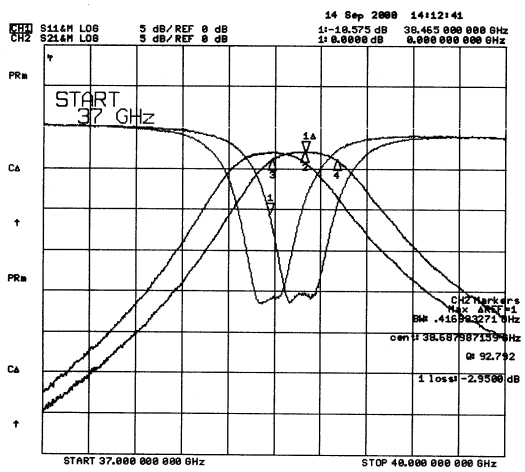

Fig. 11. Measured 2 pole filter responses at 100 Volts.

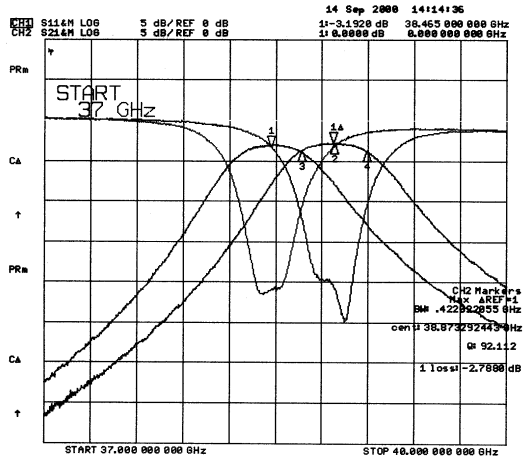

Fig. 12. Measured 2 pole filter responses at 200 Volts.

A three-pole finline filter is also designed and built at K band. Fig. 13 shows the measured response. The filter tuned from 0 to 300 Volts. 501 MHz tunability is achieved without major degradation of the filter response. The insertion loss increases only by 0.3 dB from 1.7 dB to 2.0 dB.

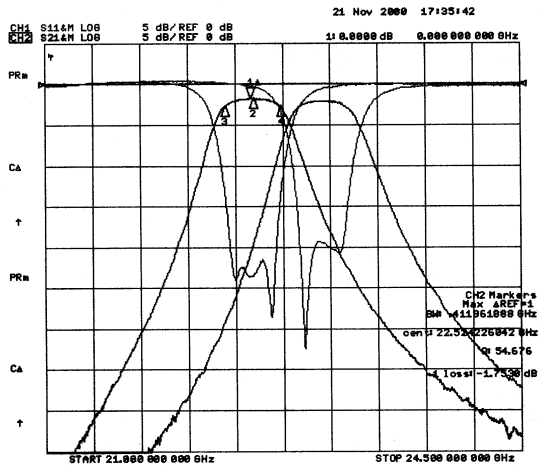

Fig. 13. 3 pole K band filter responses at 0 and 300 Volts.

IV. CONCLUSION

In this paper, a rigorous method for the finline structure tunable filter design is presented based on filter synthesis and full wave analysis using Ansoft EM simulation software HFSS. A Ka-band two-pole filter using thick film BSTO varactors is built to verify the design. Another three-pole filter at K band is also introduced. The measurement results show the good agreement with the HFSS simulations. This method can also be used for higher order tunable filter designs.

ACKNOWLEDGEMENT

The authors would like to thank Luna Chiu for her support with the material aspects of varactors and to Yongfei Zhu for many helpful discussions.

REFERENCES

[1] V.N. Keis, A.B. Kozyrev, M.L. Khazov, J. Sok and J.S. Lee, "20 GHz tunable filter based on ferroelectric (Ba,Sr) TiO3 film varactors," *IEE Electronics Letters*, vol. 34, no. 11, pp. 1107-1109, May 1998.

[2] R.J. Cameron, "Fast generation of Chebychev filter prototypes with asymmetrically-prescribed transmission zeros," *ESA Journal*, vol. 6, pp. 83-95, 1982.

[3] Matthael, G. L., Young, L., and Jones. E.M.T, " Microwave filter, Impedance-matching networks, and coupling structures." McGraw Hill, 1986.

[4] Jian Xu and Nick van Stigt, "FDTD Analysis of Mutual Coupling in the Combline Filter Design," *Proceedings of IEEE RAWCON'99*, pp.199-202, August 1998.